Interferometric assessment of clamping quality of borehole geophones

Yoones Vaezi* [1a] and Mirko van der Baan[1b]

1. Department of Physics, University of Alberta

[a]yvaezi@ualberta.ca, [b]Mirko.VanderBaan@ualberta.ca

Summary

Borehole arrays are often preferred over surface installations for hydraulic fracture monitoring of deep experiments due to proximity to the treatment zone. Borehole geophone strings are typically clamped to the observation wellbore wall using electromechanical or magnetic devices in order for them to be in close contact with the surrounding formations so as to record the background noise and propagating wavefields related to the microseismic experiments. This contact needs to be maintained throughout the recording time. We have used seismic interferometry to assess the clamping quality of borehole geophone arrays. We suggest that the characteristics of the reconstructed crosscorrelation functions between a reference receiver and other receivers in an array are indicative of the quality of clamping. The dominant contribution of tube waves in correlation functions and emergence of incoherent and fluctuating crosscorrelation functions indicate inadequate coupling while dominant appearance of clean body waves in the correlation gathers suggest a properly maintained coupling. We have applied this method to two different borehole microseismic datasets.

Introduction

Hydraulic fracture mapping remains to be the most common and notable use of microseismic monitoring in oil and gas industry. It involves the acquisition of continuous seismic data for the purpose of detecting and locating microseismic events induced by fracture treatments using three component (3C) borehole and/or surface instruments. This provides information on fractures growth and propagation and therefore allows operators to optimize stimulations, well spacing, and the overall field development and also avoid geohazards (Warpinski, 2009).

Due to proximity to the treatment zone borehole installations are often preferred over surface counterparts for hydraulic fracture monitoring of deep experiments. This is because first seismic waves emitted from microseismic events suffer much less from intrinsic attenuation and geometrical spreading when travelling shorter offsets; second the levels of surface waves, which can mask weaker and distant microseismic events, are considerably lower in deeper zones with respect to surface recordings. Therefore, using borehole geophones provides higher chance of detecting a greater number of microseismic events. However, geophones deployed in the observation well must be clamped properly to the side of the wellbore wall in order for their recorded time series to be useful. The common practice in industry for borehole monitoring of hydraulic fracture treatments is to install 6 to 12 geophones with an equidistant spacing and secure them in place with an electromechanical or magnetic device that has a clamping force to weight ratio of at least ten (St-Onge et al., 2013). The deeper the borehole array is deployed the lower the control is attained on the clamping quality, especially for deviated boreholes if the array is installed on the bending section of the wellbore. If a geophone is detached from the borehole wall

and is hanging inside the wellbore it will most likely record only tube waves propagating inside the wellbore fluid, instrument self-noise, high-frequency waves travelling within the wellbore casing, or the high-amplitude constituents of noise wavefields and signals traveling in the surrounding formations. Therefore, the detached geophones can no longer be used for analysis of seismic background noise or monitoring hydraulic fracture treatments.

Seismic interferometry (SI) in passive seismic experiments refers to a technique for reconstructing coherent part of noise, which is deeply buried into local seemingly incoherent noise, propagating between two receivers by crosscorrelating their noise records. For regional scale networks of widely separated stations, applying SI to long noise records at every station pairs in the array would result in the corresponding inter-receiver Green's function or impulse response, dominated commonly by slowly attenuated surface (Rayleigh) waves, assuming that noise source distribution is spatially homogeneous around the stations (Lobkis & Weaver, 2001; Derode et al, 2003; Shapiro & Campillo, 2004; Snieder, 2004; Wapenaar, 2004). The surface wave dispersion curves estimated from these noise correlation functions can consequently be inverted for 2D and 3D velocity structures.

Body waves may also be extracted from SI of closely-spaced receivers (Roux et al., 2005; Draganov et al., 2007; Gertstoft et al., 2008; Zhang et al., 2010; Ruigrok et al., 2011). Miyazawa et al. (2008) extracted P and S-waves from noise crosscorrelation on a vertical array deployed for monitoring steam injection into an oil reservoir. Grechka and Zhao (2012) recovered body waves and the corresponding formation velocity models nearby the wellbore from correlation of noise records at borehole geophones in different single- and cross-well acquisition geometries in microseismic monitoring experiments and for both horizontal and vertical observation wells. Their results were compatible with the existing velocity models obtained from well logs.

Following discussions with Vladimir Grechka, we explore if we can evaluate clamping quality of borehole geophones based on the wave types retrieved by SI. We propose that if the crosscorrelation functions are dominated by tube waves with a much less contribution from high amplitude constituents of signals this would mean that the clamping job might have not been done properly and the geophone array may be hanging inside the wellbore so that it records mostly tube waves. On the other hand, detection of dominant P- and S-waves on the correlation gathers confirms that the geophones are well clamped to the wellbore.

Methodology

The data processing steps involved in this method are summarized in Figure 1. Our approach for generation of crosscorrelation functions (CCFs) is similar to the scheme proposed by Bensen et al. (2007). In the first step, the mean and the linear trends are removed from the recorded time series at each station in the borehole array. They also correct for the instrument response to increase the bandwidth over which the CCFs are calculated. As crosscorrelation is a linear process, a Welch method is adopted for calculation of CCFs for which a sliding time window length and percent of overlap between successive windows should be defined (Seats et al., 2012). The window length should be chosen in such a way that it optimizes a trade-off between the fluctuations associated with a short time window and numerical computation resulting from a long time window. It should also be long enough to assure the emergence of signals of the Green's function in the single time window CCFs. A time window length similar to the duration of the dominating coherent disturbing signals (e.g., teleseismic surface waves) is expected to provide reliable results (Groos et al., 2012). CCFs converge faster and are more robust using short-duration overlapping time windows than with long, non-overlapping time windows (Seats et al., 2012). Applying a bandpass filter to each window will determine the bandwidth over which the CCFs will be calculated. Next individual windows are normalized in time domain to reduce the effect of earthquakes, non-stationary noise sources, and instrumental irregularities on CCFs (Bensen et al., 2007). The most common and effective temporal normalization methods are running absolute mean normalization and 1-bit (replacing the waveforms with their sign) normalizations

(Bensen et al., 2007; Larose et al., 2004). Spectral whitening is necessary to increase the resulting CCFs' bandwidth, prevent spectral peaks to overwhelm the CCFs, and therefore equalize the large differences in spectral amplitudes of the signals contributing to seismic noise in the analyzed frequency range (Bensen et al., 2007; Groos et al., 2012). It involves dividing the frequency spectrum of each window by its smooth version. In the next step a reference geophone is selected for the normalized crosscorrelations (crosscorrelations divided by the geometric mean of the autocorrelations functions at lag zero) to be calculated between this receiver and any other receivers in the array. Several single-time window CCFs are then stacked to obtain a final CCF with enhanced signal-to-noise ratio (SNR). The final CCF calculated between the reference receiver and any other receivers in the array simulates a response that would have been measured at each of the latter receivers if there was a source at the position of the reference receiver. This is commonly called a virtual source (Bakulin and Calvert, 2004 & 2006).
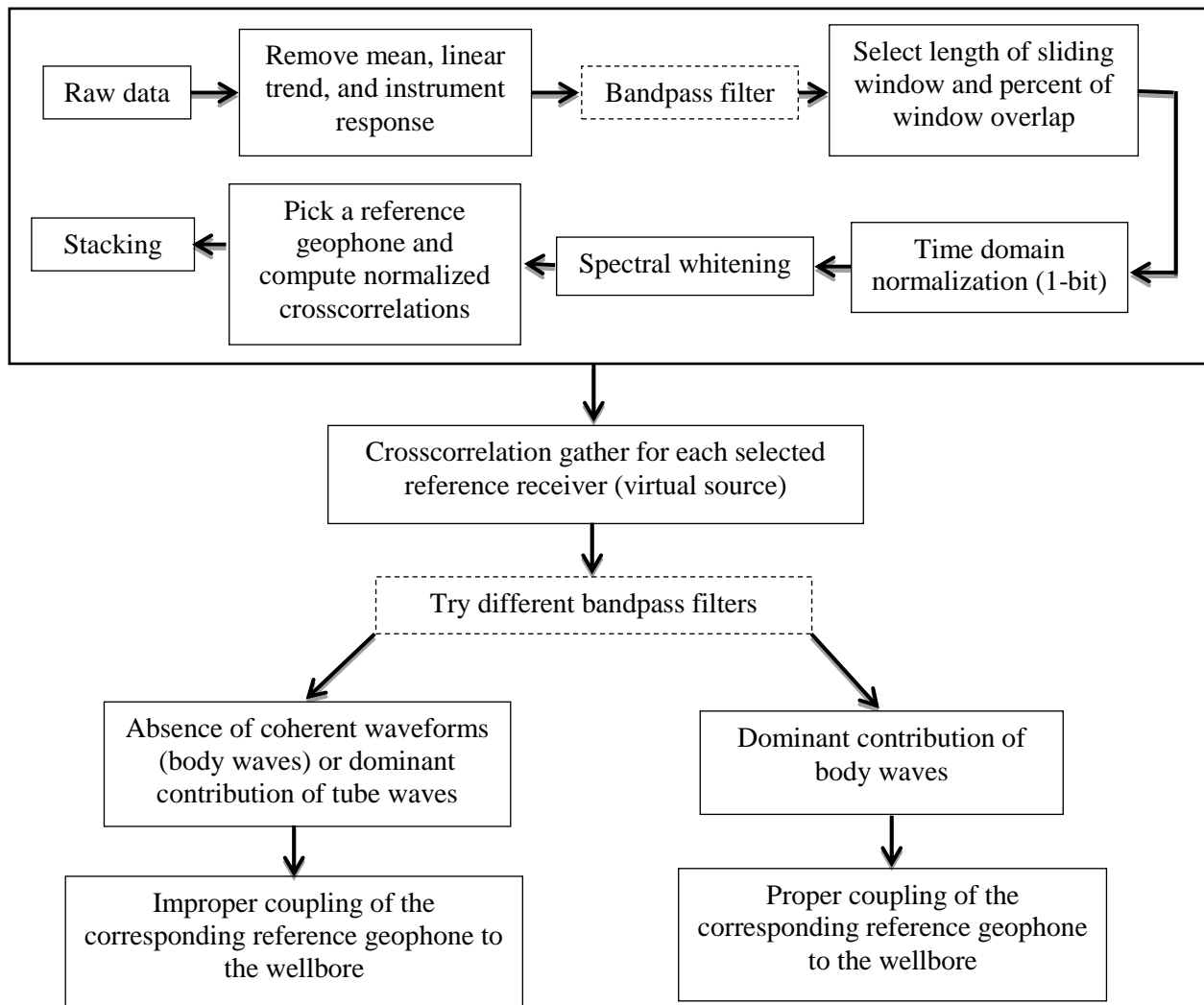

Figure 1. The processing scheme for generation of crosscorrelation functions and following steps for assessment of clamping quality of borehole geophones. The dashed boxes indicate that only one of these steps is implemented at a time.

The above processing scheme can be applied to every component and every reference receiver. If ignored prior to temporal normalization, different bandpass filters can be applied to the resulting correlation gather. We suggest that if the gather is dominated by only tube waves travelling within the

borehole fluid it could mean that the coupling of the toolstring is not properly performed. However, some high-amplitude low-frequency signals can still be recovered because they can still be sensed by a hanging array or receiver in the wellbore. Moreover, lack of coherency in the correlation gather of a reference receiver could also be interpreted by its bad coupling. On the other hand, emergence of meaningful and "clean" body waves throughout the correlation gather for quite a wide bandwidth confirms that the borehole array has maintained its attachment to the wellbore wall.

Examples

We have applied this procedure to two different borehole microseismic data which were acquired to monitor multistage fracture treatments taking place at two horizontal wells for the purpose of increasing the formation permeability of two tight gas reservoirs. The first data (Rolla Microseismic Experiment) come from a geophone array consisting of 6 3C 4.5-Hz receivers deployed in a deviated well. The array is installed in the bending portion of the observation well where the deviation angles is less than 20 degrees (Figures 2a and b). The second data are from an array in a vertical observation well composed of 12 3C receivers (Figures 2c and d).
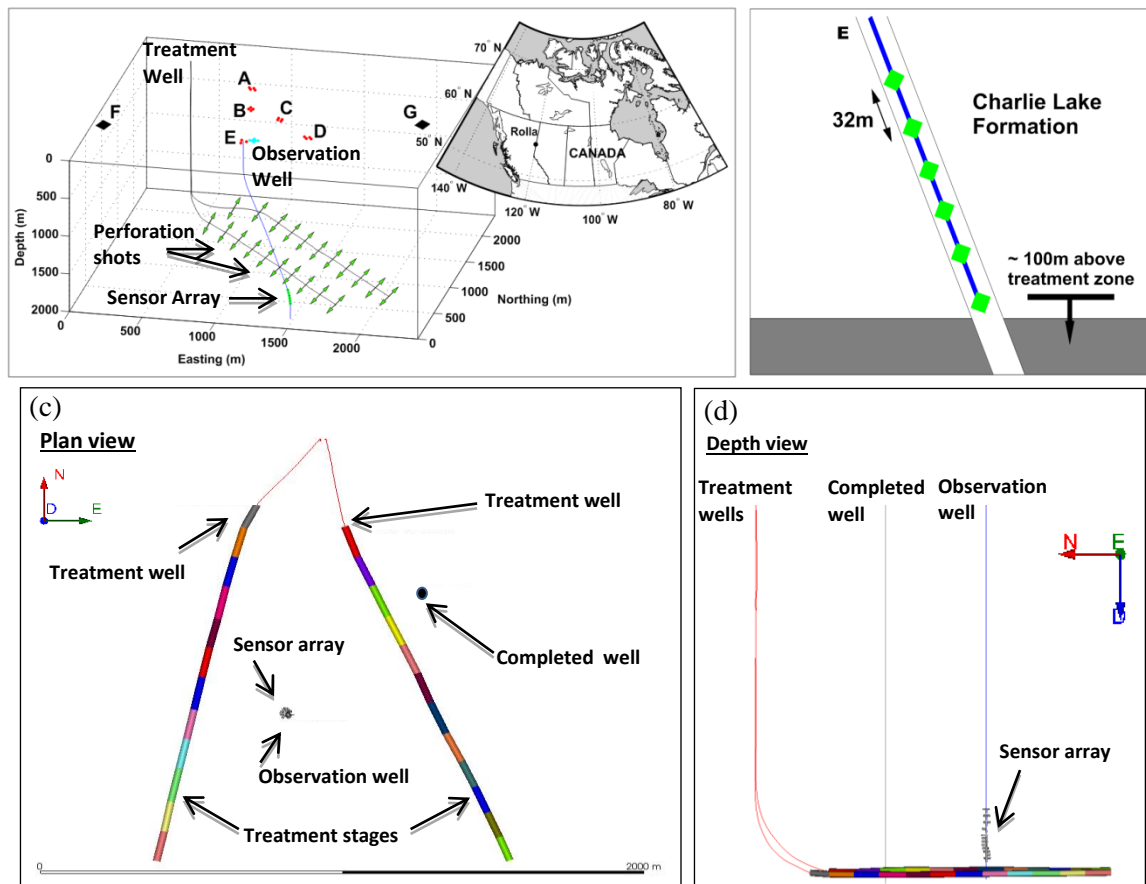
Figure 2. (a) The 3D view of the acquisition geometry of the first experiment. (b) Cross section showing borehole toolstring of six 3C geophones in the deviated observation well (modified after Eaton et al., 2013). (c) & (d) The plan and depth view of the acquisition geometry of the second microseismic experiment with the vertical borehole array consisting of 12 3C geophones.

The correlation functions calculated between the vertical component of shallowest receiver and that of any other receivers in the array for the first and second data are shown in Figures 3 and 4, respectively. Sliding time windows of 15 s and 5 s length overlapping by 50% are used to generate the CCFs for the

first and second data, respectively. In the situation where noise sources are homogeneously distributed around the receivers, SI is expected to result in a time symmetric CCF (Stehly et al., 2006). A one-sided CCF can be generated if the noise sources are dominantly located on one side of the receiver pairs (Shapiro & Campillo, 2004). The CCFs for the first data are dominated by tube waves at most of their bandwidth. Figure 3a shows the result after being band-passed by a filter with corner frequencies of [180 200 400 440] Hz. The best-fit line through the coherent arrivals (red dashed line) in this figure represents a velocity of about 1500 m/s implying that these waveforms are related to tube waves travelling down the array. Figure 3b shows the CCFs after being band-passed by a narrow filter with corner frequencies of [1 5 10 15] Hz. The best-fit line corresponds to a moveout velocity of nearly 6200 m/s which is in agreement with the P-wave velocity log in the vicinity of the array (Figure 3c) obtained by sonic log. Such high velocities are due to presence of large bodies of anhydrites, limestone, and dolomite in the formation hosting the array. These observations can be explained by the geophone array being detached from the wellbore wall. This could have been caused by the fact that compared with the straight sections, the bending sections of the wellbore provide less stability for the receivers.
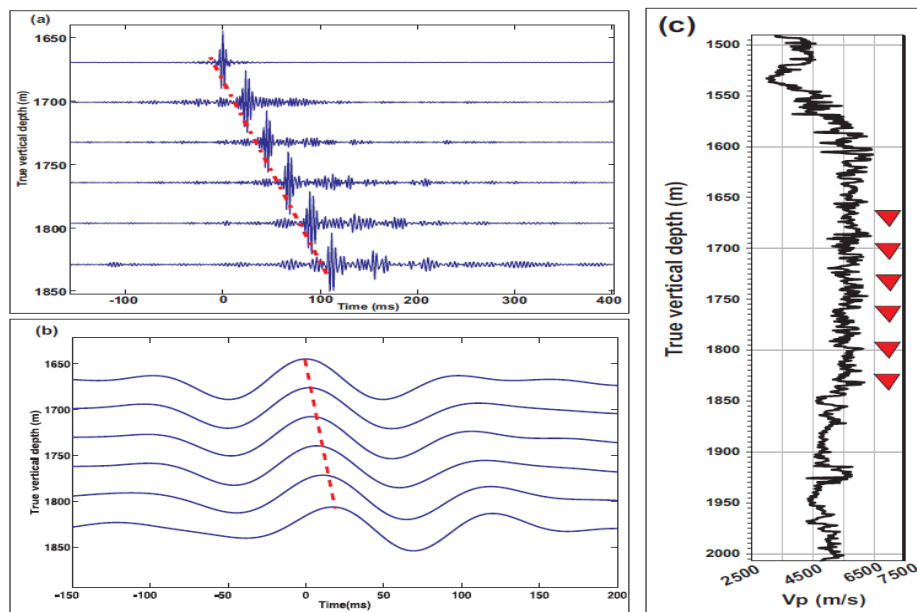
Figure 3. (a) The averaged crosscorrelation functions between the vertical component of the shallowest receiver and all other receivers in the borehole array of the first dataset after a bandpass with corner frequencies of [180 200 400 440] Hz. The move-out velocity of the reconstructed coherent and high-amplitude waveforms is approximately 1500 m/s. This suggests that these waveforms are most probably tube-waves propagating down the array and within the borehole fluid. (b) Corresponding result for frequencies of [1 5 10 15] Hz. The move-out velocity is 6200 m/s. (c) The sonic velocity log for P-waves. The high velocities suggest that the waveforms in (b) may represent a P-wave traveling down the array (Vaezi and van der Baan, 2014).

Figure 4a, on the other hand, shows the emergence of nearly time symmetric CCFs. Due to presence of large amplitude overtones of the 60-Hz electric noise peak (fundamental mode) in the raw data and CCFs, the results are low-passed below 60 Hz. The best-fit moveout velocity equals approximately 3800 m/s. A comparison of this velocity with the velocity model calculated from the sonic log (Figure 4b) confirms that these waveforms are upward and downward propagating P-waves traveling within the formation adjacent to the wellbore. Each CCF looks well correlated with one another. With these observations we suggest that the borehole array is not suffering from bad coupling.
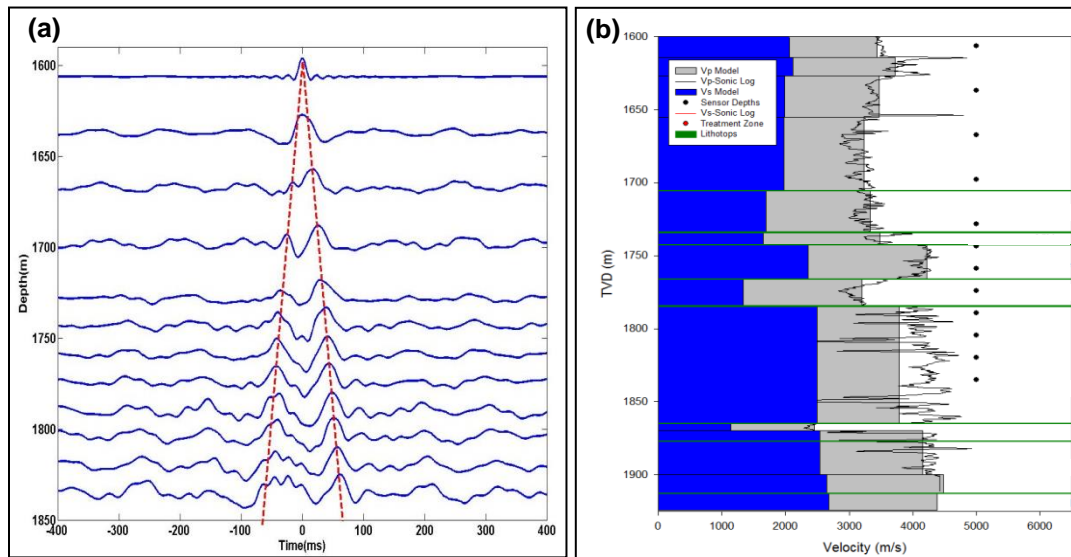
Figure 4. (a) Similar to Figure 3a but for the second dataset and after being low-passed below 60 Hz. The time symmetric responses represent a velocity around 3800 m/s. (b) The P- and S-wave velocity models initially obtained by sonic logs and then calibrated. Velocity similarities suggest that the waveforms in (a) are upward and downward propagating P-waves.

The vertical component recorders lie flat on the wellbore wall and are less prone to instability during the recording time than in horizontal sensors. One can also compute the CCFs for horizontal components as they experience more rotations and instability. The CCFs can also be calculated for every reference receiver in the array in order to better identify the incoherently behaving geophones due to their bad clamping. The resulting CCFs for such receivers will look more fluctuating.

An important factor for this method is that how fast the robust CCFs can be extracted. Having analyzed different durations of the raw data we could reconstruct the Green's function with data length of as short as 2 minutes. However, this depends strongly on the sliding time window length and overlap selections, time and frequency normalizations, distribution of sources around the receivers, and the degree of scattering.

Conclusions

We have used seismic interferometry to calculate the crosscorrelation functions between different pairs of borehole receivers in microseismic experiments. We suggest that the characteristics of the recovered waveforms can be used to assess the clamping quality of receivers to the borehole wall. We analyzed two borehole microseismic data. The dominance of the tube waves in recovered correlation gather of the first dataset can be interpreted by bad coupling of the array and its detachment from the wellbore. On the other hand, the clean P-waves appearing at all the CCFs for the second dataset confirm that it does not suffer from improper geophone coupling to the wellbore.

Acknowledgements

References

Bakulin, A., and Calvert, R., 2004, Virtual source: new method for imaging and 4D below complex overburden, *74th Annual International Meeting, SEG, Expanded Abstracts*, **23**, 2477–2480. DOI: 10.1190/1.1845233.

———, 2006, The virtual source method: Theory and case study, *Geophysics*, **71**, no. 4, SI139–SI150.

Bensen, G.D., Ritzwoller, M.H., Barmin, M.P., Levshin, A.L., Lin, F., Moschetti, M.P., Shapiro, N.M., and Yang, Y., 2007, Processing seismic ambient noise data to obtain reliable broad-band surface wave dispersion measurements, *Geophys. J. Int.,* **169,** 1239–1260, doi:10.1111/j.1365-246X.2007.03374.x.

Derode, A., Larose, E., Tantr, M., de Rosny, J., Tourin, A., Campillo, M., and Fink, M., 2003, Recovering the Green's function from field-field correlations in an open scattering medium, *J. acoust. Soc. Am.,* **113**(6), 2973–2976.

Draganov, D., Wapenaar, K., Mulder, W., Singer, J., and A. Verdel, 2007, Retrieval of reflections from seismic background noise measurements, *Geophys. Res. Lett.,* **34**, L04305, doi:10.1029/2006GL028735.

Eaton, D. W., Van der Baan, M., Tary, J-B., Birkelo, B., Spriggs, N., Cutten, S., Pike, K., 2013, Broadband microseismic observations from a Montney hydraulic fracture treatment, northeastern B.C., Canada, *CSEG Recorder*, 44–53.

Gerstoft, P., Shearer, P.M., Harmon, N., and Zhang, J., 2008, Global P, PP, and PKP wave microseisms observed from distant storms, *Geophys. Res. Lett.,* **35,** L23307, doi:10.1029/2008GL036111.

Grechka, V., and Zhao, Y., 2012, Microseismic interferometry, *The Leading Edge*, **31**, 1478-1483. DOI: 10.1190/tle31121478.1.

Groos, J.C., Bussat, S., and Ritter, J.R.R., 2012, Performance of different processing schemes in seismic noise cross-correlations, *Geophysical Journal International*, 188: 498–512. doi: 10.1111/j.1365-246X.2011.05288.x.

Larose, E., Derode, A., Campillo, M., and Fink, M., 2004, Imaging from one-bit correlations of wideband diffuse wave fields, *Journal of Applied Physics*, **95**, 8393–8399. DOI: 10.1063/1.1739529.

Lobkis, O.I. and Weaver, R.L., 2001, On the emergence of the Green's function in the correlations of a diffuse field, *J. acoust. Soc. Am.,* **110**(6), 3011–3017.

Miyazawa, M., Snieder, R., and Venkateraman, A., 2008, Application of seismic interferometry to extract P- and S-waves propagation and observation of shear-wave splitting from noise data at Cold Lake, Alberta, Canada, *Geophysics,* **73,** 35–40.

Roux, P., Sabra, K.G., Gerstoft, P., Kuperman, W.A., and Fehler, M.C., 2005, P-waves from cross correlation of seismic noise, *Geophys. Res. Lett.,* **32,** L19303, doi:10.1029/2005GL023803.

Ruigrok, E., Campman, X., and Wapenaar, K., 2011, Extraction of P-wave reflections from microseisms, *C. R. Geosci.,* **343,** 512–525, doi:10.1016/j.crte.2011.02.006.

Seats, K. J., Lawrence, J. F., and Prieto, G. A., 2012, Improved ambient noise correlation functions using Welch's method, *Geophysical Journal International*, 188: 513–523. doi: 10.1111/j.1365 246X.2011.05263.x.

Shapiro, N.M., and Campillo, M., 2004, Emergence of broadband Rayleigh waves from correlations of the ambient seismic noise, *Geophys. Res. Lett.,* **31,** L07614, doi:10.1029/2004GL019491.

Snieder, R., 2004, Extracting the Green's function from the correlation of coda waves: a derivation based on stationary phase, *Phys. Rev.,* **69,** 046610, doi:10.1103/PhysRevE.69.046610.

Stehly, L., Campillo, M., and Shapiro, N. M., 2006, A study of the seismic noise from its long-range correlation properties, *J. Geophys. Res.*, **111**, B10306, doi:10.1029/2005JB004237.

St-Onge, A., Eaton, D.W., and Pidlisecky, A., 2013, Borehole vibration response to hydraulic fracture pressure, *CSEG Geoconvention Conference*, Calgary, Alberta.

Vaezi, Y., and van der Baan, M., 2014, Analysis of instrument self-noise and microseismic event detection using power spectral density estimates, *Geophysical Journal International,* submitted.

Wapenaar, K., 2004. Retrieving the elastodynamic Green's function of an arbitrary inhomogeneous medium by cross correlation, *Phys. Rev. Lett.,* **93,** 254301, doi:10.1103/PhysRevLett.93.254301.

Warpinski, N.R., 2009, Microseismic monitoring: inside and out, *Journal of Petroleum Technology*, **61**, 80–85. DOI: 10.2118/118537-MS.

Zhang, J., Gerstoft, P., and Shearer, P.M., 2010, Resolving P-wave traveltime anomalies using seismic array observations of oceanic storms, *Earth planet. Sci. Lett.,* **292,** 419–427, doi:10.1016/j.epsl.2010.02.014.